MINISTRY OF EDUCATION AND TRAINING
VIETNAM ACADEMY OF SCIENCE AND TECHNOLOGY

GRADUATE UNIVERSITY OF SCIENCE AND TECHNOLOGY

Nguyen Hai Yen

SYNTHESIS OF GRAPHENE AND GRAPHENE QUANTUM DOTS FOR ENHANCING THE PHOTOCATALYTIC PROPERTIES OF TiO_2

SUMMARY OF DISSERTATION ON MATERIALS SCIENCE

Major: Optical, Optoelectronic, and Photonic Materials
Code: 9440127

HaNoi – 2025

The dissertation is completed at: Graduate University of Science and Technology, Vietnam Academy Science and Technology

Supervisors:

1. Supervisor 1: Assoc. Prof. Dr. Nguyen Cao Khang
   Hanoi National University of Education (HNUE)
2. Supervisor 2: Dr. Bui Hung Thang
   Institute of Materials Science

Referee 1:

Referee 2:

Referee 3:

The dissertation is examined by Examination Board of Graduate University of Science and Technology, Vietnam Academy of Science and Technology at…….(time, date…….)

The dissertation can be found at:

1. Graduate University of Science and Technology Library
2. National Library of Vietnam

INTRODUCTION

In recent decades, environmental pollution particularly water contamination caused by the persistence of hazardous organic compounds such as industrial dyes has emerged as a serious global challenge. This situation not only poses serious threats to human health but also leads to the severe degradation of natural ecosystems. In response to this reality, the research and development of efficient, sustainable, and environmentally friendly wastewater treatment technologies have become one of the top priorities in modern materials science and environmental engineering. Among various wastewater treatment methods, the use of semiconductor materials with photocatalytic activity particularly titanium dioxide (TiO_2) has been demonstrated to be a highly promising approach due to its ability to generate strong oxidative radicals such as hydroxyl (•OH), which can completely degrade organic compounds into CO_2 and H_2O. In addition, TiO_2 is a safe, non-toxic material; the byproducts produced during the degradation process are environmentally friendly, and the material itself is relatively low-cost. However, a major limitation of TiO_2 is its wide band gap (approximately 3.2 eV for the anatase phase), which restricts its photocatalytic activity to the ultraviolet (UV) region. This poses a significant drawback, as UV radiation accounts for only about 4%–5% of the total solar spectrum reaching the Earth's surface. As a result, the application of TiO_2 for environmental remediation under sunlight is significantly limited. To more effectively harness solar radiation particularly in the visible light region an important approach involves narrowing the band gap of TiO_2 to broaden its light absorption range and enhance photocatalytic efficiency. In addition, the photogenerated electron–hole pairs in TiO_2 tend to recombine rapidly, which reduces the quantum efficiency of the photocatalytic process. Therefore, to improve the efficiency of the photocatalytic process, it is essential to suppress the recombination of electron–hole pairs and simultaneously reduce

the band gap of the material. To overcome these limitations, various strategies have been explored, such as doping with metal or non-metal elements, or combining TiO_2 with conductive materials like graphene and graphene quantum dots (GQDs). Among these approaches, the formation of TiO_2/graphene and TiO_2/GQDs composites has been demonstrated to offer superior performance by enhancing visible-light absorption, suppressing electron–hole recombination, and improving charge transport efficiency. In particular, graphene quantum dots (GQDs) are a new generation of nanomaterials that exhibit strong quantum confinement effects, large surface area, excellent photoluminescence, and high biocompatibility. The integration of TiO_2 with GQDs can result in hybrid materials with high Sphotocatalytic activity under visible light, offering great potential for applications in water treatment, sensing, and energy storage.

In addition, doping the composite system with transition metal ions such as Fe, Co, Ni, and Mn can effectively tune the band gap, thereby enhancing the photocatalytic efficiency under solar irradiation.

Motivated by the outstanding advantages and versatile applications of TiO_2-based nanostructured materials particularly composite systems such as TiO_2/graphene, TiO_2/GQDs, and TiO_2/GQDs doped with transition metal ions (Fe, Co, Ni, Mn) we have selected this topic for our research: '**Synthesis of Graphene and Graphene Quantum Dots for Enhancing the Photocatalytic Properties of TiO_2".**

Research Objectives:

1. To successfully synthesize TiO_2, graphene, graphene quantum dots (GQDs), and a series of composite materials including TiO_2/graphene, TiO_2/GQDs, and TiO_2/GQDs doped with transition metal ions (Fe, Co, Ni, Mn) using ultrasonic, hydrothermal, microwave, and sol-gel methods. The research aims to optimize the material structures and improve their optical properties, thereby enhancing photocatalytic efficiency.

2. To investigate the correlations between structure, morphology, optical properties, and photocatalytic performance of the synthesized material systems, particularly in the photodegradation of methylene blue (MB) under ultraviolet and visible light irradiation.

3. To evaluate the influence of the mass ratio between TiO_2 and graphene or GQDs, as well as the effect of doped metal elements on light absorption, the efficiency of organic pollutant degradation, and the photocatalytic reaction mechanism.

Subjects of the Study:

- Nanostructured semiconductor materials, including anatase-phase TiO_2, graphene, and graphene quantum dots (GQDs).
- Composite material systems including TiO_2/graphene, TiO_2/GQDs, and TiO_2/GQDs doped with metal ions (Fe, Co, Ni, Mn).

Research Methodology

The dissertation employed experimental methods, with materials synthesized via ultrasound, hydrothermal, microwave, and sol-gel techniques. All procedures were conducted at the Institute of Materials Science and the Center for Nanoscience and Technology, Hanoi National University of Education

Structure and Content of the Dissertation

In addition to the Introduction which presents the research background, scientific significance, and rationale for selecting the topic—and the General Conclusion, which summarizes the main findings, the dissertation is structured into four main chapters as follows:

Chapter 1. Overview of TiO_2 and Graphene Materials.

Chapter 2. Experimental Techniques.

Chapter 3. Investigation of Selected Properties of TiO_2/Graphene Composite Materials.

Chapter 4. Synthesis of Graphene Quantum Dots, TiO_2-Based Composites, and TiO_2 Doped with Fe, Co, Ni, Mn/GQDs, and Investigation of Their Selected Properties.

The Conclusion and Recommendations section summarizes the key research findings, draws scientific and practical conclusions, and proposes directions for future studies. The dissertation ends with a list of publications directly related to the research content.

Chapter 1. OVERVIEW OF TiO_2 AND GRAPHENE MATERIALS

1.1. Overview of TiO_2 Materials

TiO_2 is a widely used semiconductor with a large band gap (~3.2 eV for anatase), limiting its activity to UV light, which comprises only 4–5% of the solar spectrum. Under UV irradiation, TiO_2 generates electron–hole (e^-/h^+) pairs that produce reactive species (e.g., •OH radicals) capable of degrading organic pollutants. However, its photocatalytic efficiency is hindered by limited light absorption and rapid charge recombination. To overcome these limitations, TiO_2 can be modified through combination with conductive materials such as graphene or GQDs, or by metal doping, to broaden its light response and enhance pollutant degradation.

1.2. Overview of Graphene Materials

Graphene is a two-dimensional material consisting of a single layer of carbon atoms arranged in a hexagonal lattice. It exhibits exceptional mechanical strength, outstanding electrical conductivity, excellent thermal conductivity, and is nearly transparent.

When combined with TiO_2, graphene enhances charge transport and suppresses electron–hole recombination, thereby improving photocatalytic efficiency.

Graphene is considered the fundamental structural unit from which various carbon allotropes are derived, such as fullerenes, carbon nanotubes, and graphite. When a graphene sheet is rolled into a sphere, it forms a

fullerene (zero-dimensional, 0D); when rolled into a cylinder, it forms a carbon nanotube (one-dimensional, 1D); and when stacked in multiple layers, it reconstructs the three-dimensional structure of graphite (3D). (Figure 1.1.)

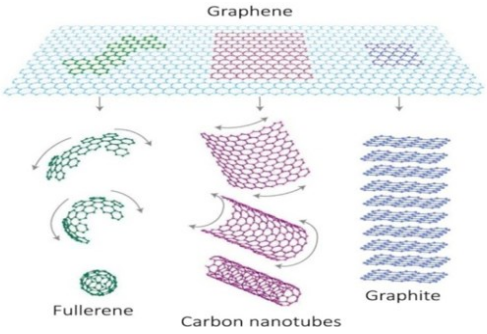

Figure 1.1. Various Structural Forms of Graphene.

Graphene consists of a single layer of carbon atoms arranged in a two-dimensional hexagonal lattice, with a C–C bond length of approximately 0.142 nm. Each carbon atom forms three strong in-plane sp^2 covalent bonds, along with delocalized π-bonds originating from the out-of-plane pz orbitals, which together contribute to its exceptional electrical conductivity. This unique two-dimensional structure is the key to graphene's superior mechanical, thermal, and optical properties compared to other carbon allotropes. (Figure 1.2.)

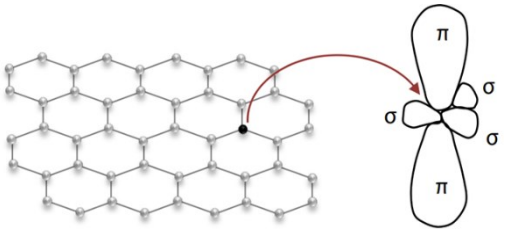

Figure 1.2. Structure of Graphene.

1.3. Overview of Graphene Quantum Dots (GQDs)

Graphene quantum dots (GQDs) are graphene-based nanoparticles with sizes below 20 nm, exhibiting quantum properties such as exciton confinement and broadband photoluminescence, ranging from ultraviolet to infrared. GQDs are chemically inert, biocompatible, easily synthesized, and possess low toxicity, making them well-suited for applications in biomedicine, energy, sensing, and catalysis. Their optical properties depend on particle size, surface functional groups, and synthesis conditions.

GQDs can be synthesized via top-down approaches (cutting larger graphene structures) or bottom-up methods (from small molecular precursors), including hydrothermal, microwave-assisted, chemical, and pyrolytic techniques. They possess high photoluminescence quantum yield, which can be tuned according to specific application requirements, particularly in photocatalysis and sensing. Compared to heavy metal-based quantum dots, GQDs offer significant advantages and are emerging as promising materials for widespread applications in nanotechnology and environmental technologies.

1.4. Overview of TiO_2/Graphene Composite Materials

TiO_2 is a powerful photocatalyst; however, its wide band gap restricts light absorption to the ultraviolet region, leading to limited solar energy utilization. Integrating TiO_2 with graphene significantly enhances its photocatalytic performance through three primary mechanisms: (1) increased adsorption of pollutants, (2) improved charge separation and transport, and (3) expanded light absorption into the visible range. Graphene acts as an electron acceptor, promoting electron–hole separation and suppressing recombination due to its lower Fermi level and high electron mobility. Additionally, the formation of Ti–O–C bonds at the interface between TiO_2 and graphene contributes to narrowing the band gap and enhancing light absorption in the 400–410 nm range. The photocatalytic degradation efficiency of pollutants such as methylene blue is significantly

higher for TiO_2/graphene composites than for pure TiO_2. The photocatalytic properties of the composites are strongly influenced by the synthesis method—such as sol-gel, hydrothermal, or microwave techniques—and the nature of the precursors used.

Summary of Chapter 1

This chapter provided an overview of research on TiO_2, graphene, graphene quantum dots (GQDs), and TiO_2/graphene composite materials aimed at improving photocatalytic performance. While TiO_2 exhibits strong photocatalytic activity, its effectiveness is limited by its UV-only light absorption. In contrast, graphene and GQDs offer high electrical conductivity, photoluminescence, and adsorption capacity. The integration of TiO_2 with graphene expands the light absorption range, enhances charge separation efficiency, and improves pollutant degradation capability. This dissertation focuses on the synthesis and characterization of TiO_2/graphene-based composites for environmental remediation applications.

Chapter 2. EXPERIMENTAL TECHNIQUES

2.1. Synthesis Procedure

2.1.1. *Synthesis Procedure of TiO_2 Material*

TiO_2 was synthesized via the sol-gel method using titanium isopropoxide [$Ti(OC_3H_7)_4$, TTIP] as the precursor

The procedure includes the following steps: Hydrolysis of TTIP in an acidic or basic medium. Aging of the resulting gel followed by calcination at temperatures ranging from 400 to 800 °C to obtain anatase and rutile phases.

2.1.2. *Synthesis Procedure of Graphene*

Graphene was synthesized from graphite using high-power ultrasonication. Graphite was dispersed in a suitable solvent and subjected to high-frequency ultrasonic treatment. After several hours of sonication, graphene layers were exfoliated from the graphite structure.

Graphene was synthesized via an electrochemical exfoliation method using high-purity graphite rods and subsequently functionalized with carboxyl (-COOH) groups to improve its dispersibility in solvents. The functionalization process was carried out by treating the graphene with a mixed acid solution of HNO_3 and H_2SO_4 in a 1:3 volume ratio at 70 °C for 5 hours. The resulting product, after being filtered and neutralized to pH ~7, exhibited good dispersibility or could be dried under ambient conditions.

2.1.3. *Synthesis procedure of graphene quantum dots (GQDs)*

GQDs were synthesized from citric acid (CA) via microwave-assisted pyrolysis, followed by a hydrothermal treatment at 220 °C for 16 hours.

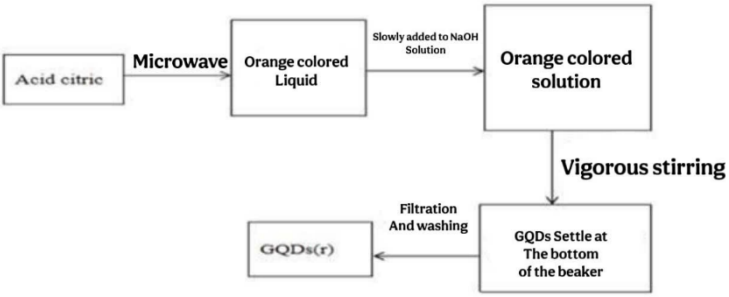

Figure 2.1. Synthesis procedure of graphene quantum dots (GQDs).

The optimal synthesis conditions were identified as a microwave power of 800 W and a solution pH of 11.

2.1.4. *Synthesis procedure of TiO_2/graphene and TiO_2/GQDs nanocomposites*

TiO_2/graphene composite: The components were mixed in a specific ratio, followed by ultrasonic-assisted dispersion, then dried and mildly annealed. TiO_2/GQDs composite: Similarly, GQDs were added to the TiO_2 precursor solution prior to gel formation Figure 2.2.

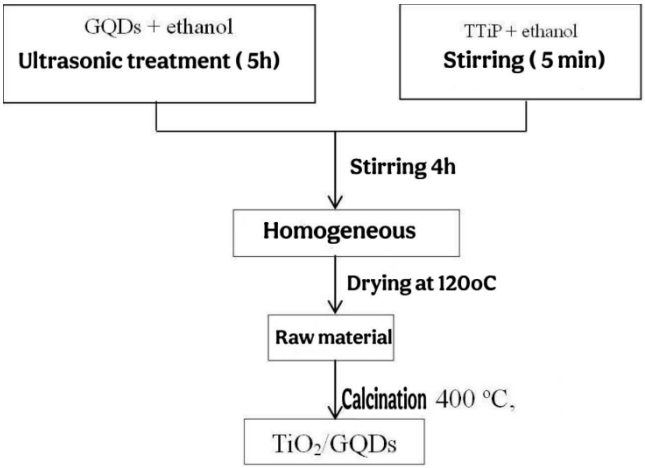

Figure 2.2. Synthesis procedure of the TiO_2/GQDscomposite material.

2.1.5. ***Synthesis procedure of Fe, Co, Ni, and Mn-doped TiO_2/graphene quantum dots (GQDs) composite material with a 1:20 ratio***

Metal salts were added to the TiO_2/GQDs mixture at varying weight ratios (4–12%) with the aim of tuning the band gap and enhancing catalytic activity.

2.1.6. ***Methylene blue degradation procedure***

The photocatalytic activity was evaluated by monitoring the degradation of methylene blue (MB) solution (10 ppm) under light irradiation using TiO_2/graphene samples. The experimental procedure included a dark adsorption phase, followed by hourly illumination. Samples were collected at regular intervals, and the residual MB concentration was determined by measuring the UV–Vis absorption spectra. Prior to measurement, all samples were centrifuged to remove any solid precipitates.

2.2. Characterization methods of material structure and properties

XRD was used to identify crystal phases and estimate nanoparticle size. Raman spectroscopy analyzed carbon structure and confirmed the presence of graphene and GQDs. UV–Vis spectra determined the optical

band gap, while FTIR identified functional groups. PL spectroscopy evaluated electron–hole recombination. BET analysis provided surface area and pore size data. SEM revealed morphology and particle size, and zeta potential measurements assessed colloidal stability.

Chapter 2 Conclusion

We selected simple and cost-effective synthesis methods suitable for the technical and economic conditions of laboratories in Vietnam to fabricate TiO_2, graphene, GQDs, and their related composites. These procedures ensured that the resulting materials met the quality standards required for fundamental research. Characterization techniques such as SEM, BET, FTIR, XRD, Raman, and UV–Vis spectroscopy were employed to analyze the structural, optical, and photocatalytic properties of the materials, all of which can be readily conducted domestically.

Chapter 3. CHARACTERIZATION OF THE TiO_2/GRAPHEN COMPOSITE

3.1. Characterization of TiO_2 Material

3.1.1. *Crystal Structure of TiO_2*

The synthesized TiO_2 mainly exhibited the anatase phase, with phase composition influenced by pH and calcination temperature. At 800 °C, the rutile content increased. Anatase generally shows superior photocatalytic activity to rutile.

XRD results show that both pH and calcination temperature significantly influence the crystal structure and phase transitions of TiO_2. At pH = 2, 800 °C promotes the transformation from anatase to rutile, while at pH = 4, rutile does not form under the same condition. Brookite appears only at pH = 4 and 400 °C, indicating a strong dependence on synthesis conditions. Figures 3.1 and 3.2 confirm the presence of anatase, brookite, and rutile phases. Crystallite sizes (6–26 nm), calculated by the Debye–Scherrer equation, show little variation in lattice constants. Pseudo-Voigt

fitting reveals 26.23% brookite in T4-400 and 23% rutile in T2-800, which directly affect photocatalytic efficiency under visible light.

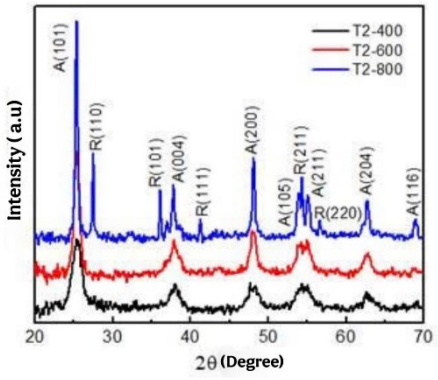

Figure 3.1. XRD patterns of TiO_2 samples synthesized at pH = 2 and calcined at 400 °C, 600 °C, and 800 °C.

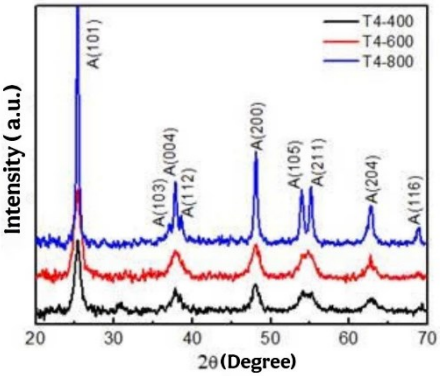

Figure 3.2. XRD patterns of TiO_2 samples synthesized at pH = 4 and calcined at 400 °C, 600 °C, and 800 °C.

3.1.2. *Raman and UV–Vis Absorption Spectra of TiO_2 Material*

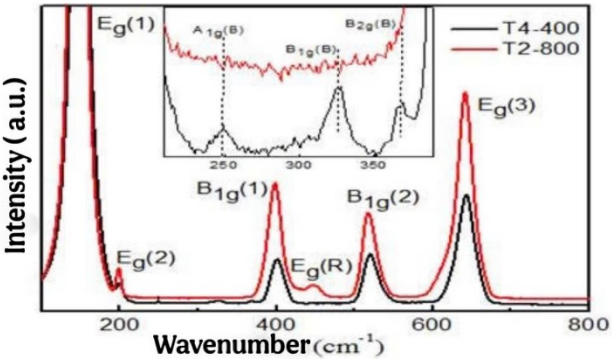

Figure 3.3. Raman spectra of samples T4-400 and T2-800.

The Raman spectrum of sample T4-400 exhibits characteristic vibrational modes of the anatase phase, along with weak peaks in the 220–380 cm^{-1} range, confirming the presence of brookite, in agreement with XRD results.

Sample T2-800 shows typical anatase peaks and an additional weak band at 448 cm^{-1}, indicative of the rutile phase. Raman bands associated with

Ti–Ti and Ti–O vibrations further confirm the crystal structure and phase composition of the synthesized TiO_2 samples.

The absorption spectra of TiO_2 samples show strong absorption in the UV region. The optical band gap (Eg) was estimated using Tauc plot extrapolation. Samples T2-400 and T2-600 exhibited similar Eg values (~3.2 eV), corresponding to the anatase phase, while T2-800 showed a reduced Eg of 3.1 eV due to the presence of rutile. The red-shift in the absorption edge of T2-800 reflects the influence of phase transition on optical properties.

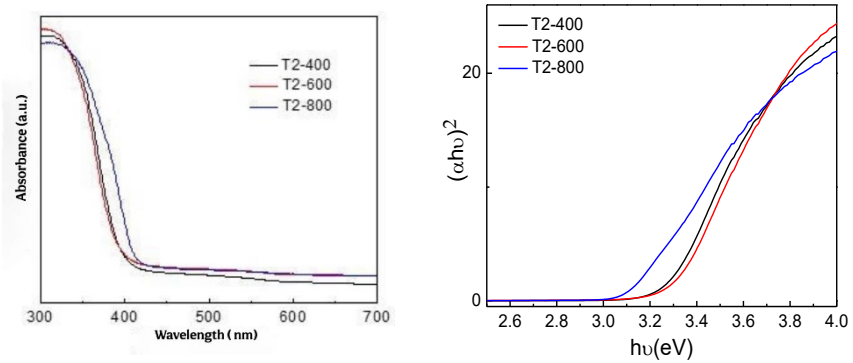

Figure 3.4. UV–Vis absorption spectra of TiO_2 samples: (a) as a function of wavelength and (b) as a function of photon energy.

3.1.3. *Photocatalytic Properties of TiO_2 Material*

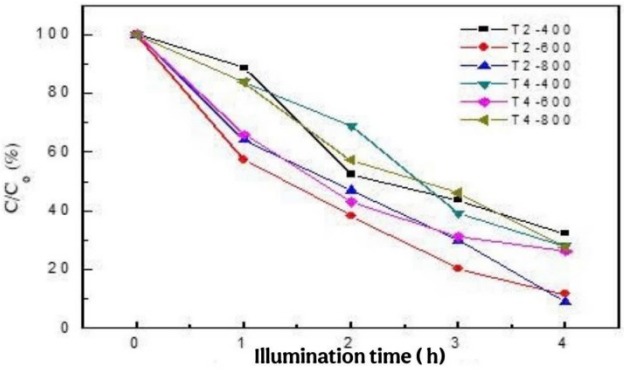

Figure 3.5. Time-dependent degradation of methylene blue by TiO_2 samples.

The photocatalytic performance of the TiO_2 samples was evaluated through the degradation of methylene blue (MB) under UV irradiation, revealing that all samples exhibited a clear degradation trend over irradiation time

Sample T2-800 achieved the highest degradation efficiency (90%), attributed to the coexistence of anatase and rutile phases. This multiphase combination enhances charge separation by suppressing e^-/h^+ recombination and promotes the generation of reactive oxygen species such as •OH and $•O_2^-$. As methylene blue (MB) is a persistent organic compound, this result demonstrates the high photocatalytic efficiency of the synthesized material.

3.2. Graphene Material

3.2.1. *Surface Morphology*

FESEM images reveal that the size of graphite flakes gradually decreases and becomes more uniform with increasing ultrasonic treatment time from 1 to 5 hours. After 5 hours, the resulting material consists of few-layer graphene, confirming the effectiveness of high-power ultrasonication in exfoliating graphite. The exfoliation mechanism is attributed to the formation and collapse of microscopic cavitation bubbles in the liquid medium, which disrupt the Van der Waals forces between graphene layers..

3.2.2. *Raman Spectroscopy, Particle Size, and Colloidal Stability*

The Raman spectrum displays characteristic peaks of graphene, with the 2D band becoming more symmetric and the I_{2D}/I_G ratio reaching 0.46 after 5 hours of ultrasonication, indicating the formation of multilayer graphene (more than five layers). The increasing I_D/I_G ratio with sonication time reflects rising structural disorder due to defects; however, the calculated

Lα, L_D, and n_D values suggest that the defect density remains low (1.4–2.6 × 10^{11} cm^{-2}). This confirms that the obtained graphene possesses a stable structure and is only slightly affected by surface modification.

Particle size distribution and zeta potential analysis indicate that 5-hour ultrasonication is the optimal condition for producing well-dispersed and stable graphene, with lateral sizes mainly in the 200–400 nm range and an average thickness of ~3.27 nm (fewer than 10 layers). FESEM and TEM images confirm the presence of few-layer graphene flakes with sharp edges and low defect density.

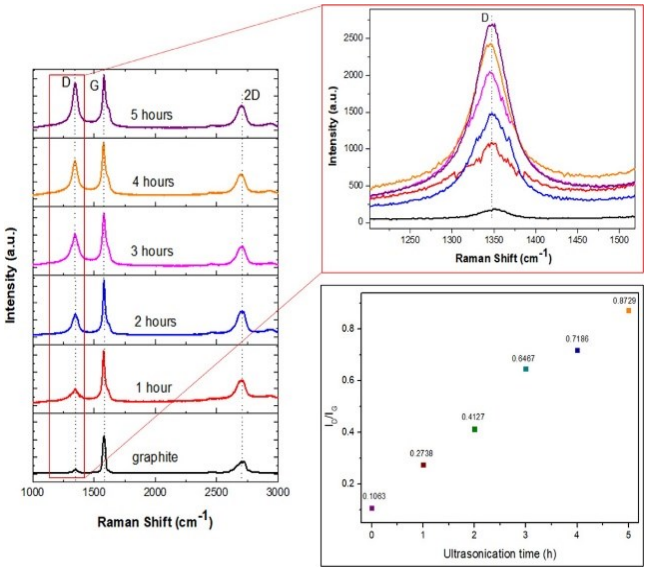

Figure 3.6. Raman spectra of graphite at different ultrasonication times.

The zeta potential reaches ~30 mV, and the suspension remains stable after 5 months of storage, indicating high physical stability. The exfoliation yield averaged 81.5% over five repetitions, demonstrating the method's reliability and strong potential for practical application.

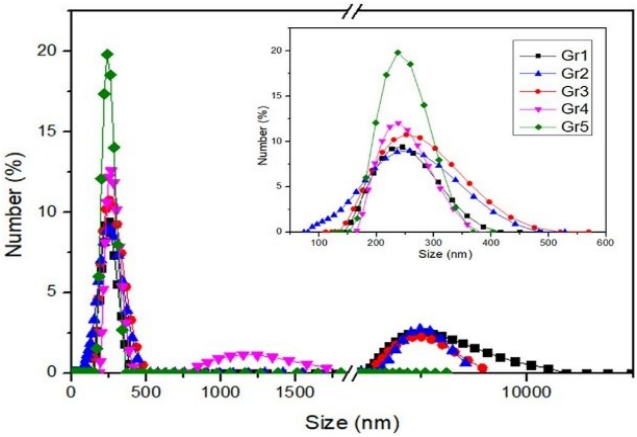

Figure 3.7. Size distribution of graphene at different ultrasonication times.

3.3. TiO_2/Graphene Composite System

3.3.1. ***Structure and Morphology***

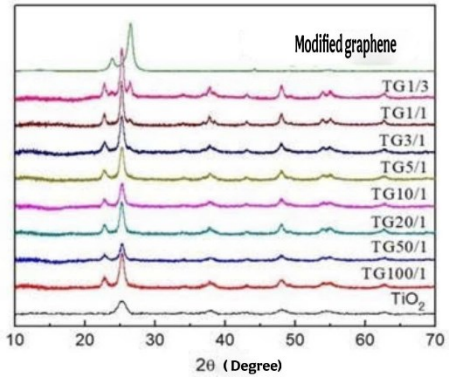

Figure 3.8. XRD patterns of the TiO_2/graphene composite samples.

The XRD patterns of TiO_2/graphene samples confirm the presence of the anatase phase and the (002) diffraction peak of graphene in samples with higher graphene content.

Calcination at 400 °C facilitates the reduction of GO to graphene, improving the structural integrity and electrical conductivity of the composite. The diffraction peak around 43° suggests the possible presence

of a small amount of residual graphite that was not fully exfoliated.SEM images of the TiO_2/graphene composites show that spherical TiO_2 nanoparticles, with an average size of 20–30 nm, are distributed across the graphene surface, indicating good interfacial contact between the two phases. The observed particle size is larger than that estimated from XRD, suggesting a polycrystalline structure of TiO_2. In the TG10/1 sample, particle agglomeration is observed due to the low graphene content, which is insufficient to prevent TiO_2 aggregation. This indicates that the TiO_2-to-graphene ratio significantly affects the dispersion and structural stability of the composite material.

3.3.2. *FTIR, UV–Vis, and PL Analyses*

FTIR: The appearance of C=C, C–O, and Ti–O bands confirms the formation of TiO_2–graphene bond. UV–Vis: The composite exhibits enhanced light absorption in the visible region. PL: The reduced photoluminescence intensity indicates suppressed electron–hole recombination.

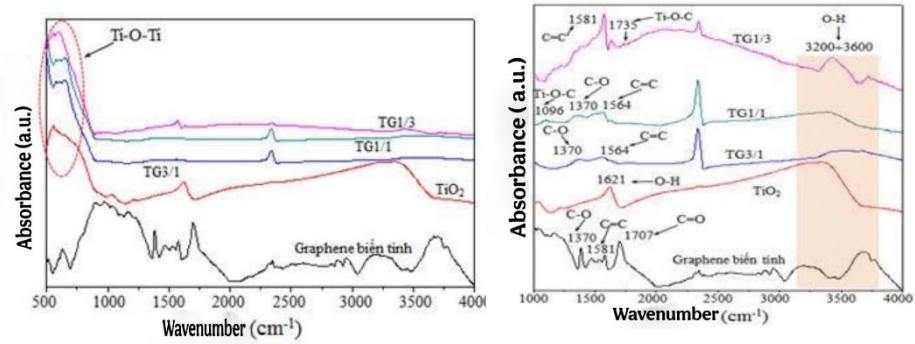

Figure 3.9. FTIR spectra of TiO_2, functionalized graphene, and TiO_2/graphene composites recorded in two wavelength ranges: (a) 500–4000 nm and (b) 1000–4000 nm.

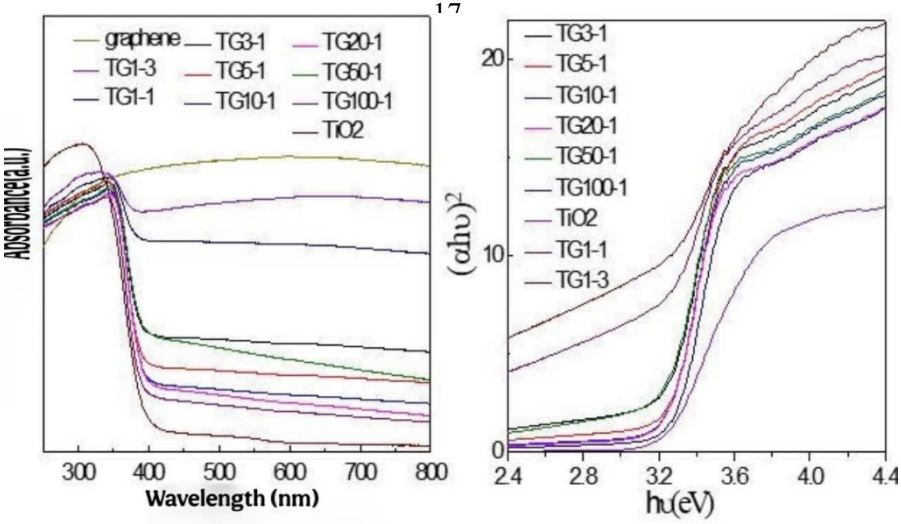

Figure 3.10. Absorption spectra of the TiO_2/graphene system as a function of wavelength and photon energy.

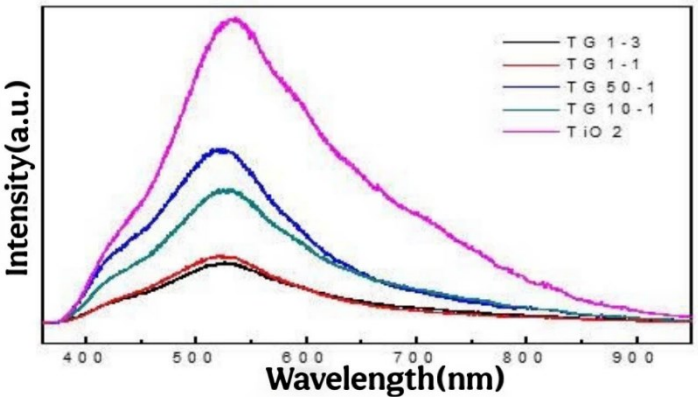

Figure 3.11. Photoluminescence spectra of TiO_2 and TiO_2/graphene materials.

3.3.3. *Photocatalytic Properties of TiO_2/Graphene Materials*

The photocatalytic efficiency of TiO_2/graphene samples under visible light was significantly higher than that of pure TiO_2. Among them, sample TG1/3 exhibited the best performance, with only 47.23% of methylene blue (MB) remaining after 4 hours. The incorporation of graphene enhances adsorption, electrical conductivity, and charge carrier lifetime by reducing

electron–hole recombination. A 100 W incandescent lamp was used as the light source, simulating realistic lighting conditions. The improved performance is attributed to the role of graphene as an electron acceptor, which facilitates more effective charge separation within the composite system.

Chapter 3 Conclusion

This chapter has detailed the synthesis and characterization of TiO_2/graphene composite materials with the aim of improving photocatalytic performance under visible light irradiation. Both TiO_2 and graphene were successfully prepared with optimized structural and functional properties. The incorporation of graphene effectively reduced the band gap and enhanced charge carrier separation. Among the tested samples, the TG1/3 composite exhibited the highest photocatalytic activity, achieving 52.77% degradation of methylene blue after 4 hours of illumination. These findings demonstrate the strong potential of TiO_2/graphene composites for environmental remediation under natural light exposure.

Chapter 4. SYNTHESIS OF GRAPHENE QUANTUM DOTS, TiO_2 BASED COMPOSITES, AND Fe, Co, Ni, Mn- DOPED TiO_2/GQDs MATERIALS AND INVESTIGATION OF THEIR OPTICAL PROPERTIES

4.1. Study on the Influence of Fabrication Process on the Optical Properties of Graphene Quantum Dots

Graphene quantum dots (GQDs) were synthesized from citric acid via a combined microwave-assisted and hydrothermal method. The optimized conditions included microwave irradiation at 800 W for 4 minutes, a solution pH of 11, hydrothermal treatment at 220 °C, and a reaction time of 16 hours. These parameters significantly influenced the intensity and position of the photoluminescence (PL) emission of the GQDs. PL intensity increased with both pH and reaction duration, reaching a maximum under alkaline

conditions after 16 hours. The results provide a basis for tuning the optical properties of GQDs for potential applications in sensing and photocatalysis.

Optimized conditions for highly fluorescent GQDs:

- Microwave irradiation of citric acid for 4 minutes at 800 W
- NaOH solution adjusted to pH = 11
- Hydrothermal temperature: 220 °C
- Hydrothermal duration: 16 hours

4.2. Investigation of the Effect of TiO_2-to-GQDs Mass Ratio on the Photocatalytic Properties of TiO_2/GQDs Composites

4.2.1. *UV–Vis Absorption and Raman Spectra*

TiO_2/GQDs composites synthesized with different molar ratios exhibited slight shifts in the UV–Vis absorption edge compared to pure TiO_2, with absorption still centered around 400 nm. The optical band gap (Eg) of the composites decreased slightly, most notably in the TG1/1 sample, which showed an Eg of 2.88 eV. These results indicate that GQDs significantly influence the electronic structure of the composites, contributing to band gap narrowing. *Figure 4.1.*

The Raman spectra of TiO_2/GQDs composites clearly display the characteristic peaks of the anatase phase, with vibrational modes associated with Ti–Ti and Ti–O bonding.

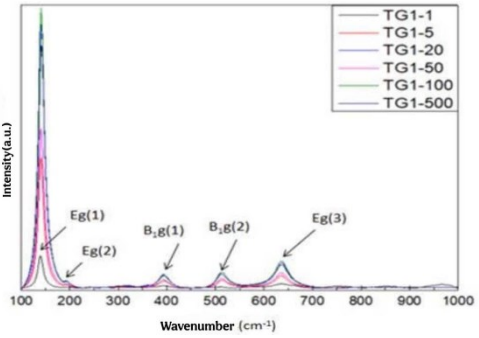

Figure 4.1. Absorption spectra and band gap energies of TiO_2/GQDs composites with different ratios.

Notably, the intensity of the Eg(1) mode (~147 cm^{-1}) varies with the GQDs ratio, being strongest in the TG1-500 sample and weakest in TG1-1, indicating a significant influence of GQDs on the crystal lattice structure. These results confirm the successful incorporation of GQDs into the TiO_2 matrix. *Figure 4.2.*

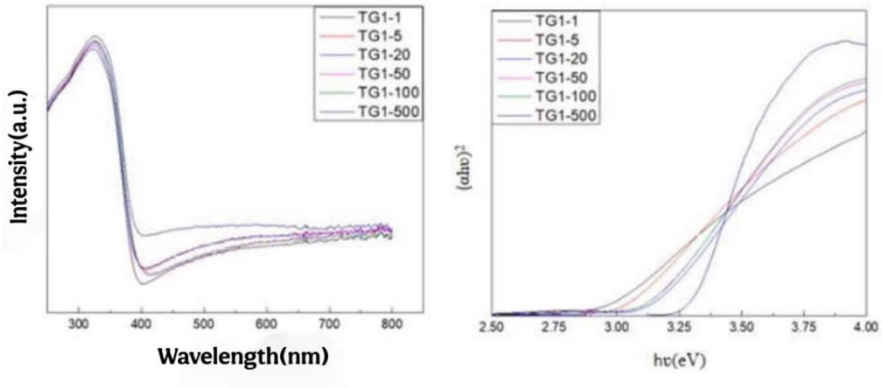

Figure 4.2. Raman spectra of TiO_2/GQDs composites with different ratios.

4.2.2. *Photocatalytic Properties of TiO_2/GQDs Composites*

The photocatalytic activity of TiO_2/GQDs composites under visible light was significantly enhanced compared to pure TiO_2. Among the samples, TG1-20 exhibited the highest efficiency, with 65.23% of methylene blue (MB) remaining after 4 hours of illumination. GQDs contributed to improved adsorption capacity, enhanced electrical conductivity, and facilitated charge separation. Photoexcited electrons from the conduction band of TiO_2 were efficiently transferred to GQDs, thereby suppressing electron–hole recombination. These results demonstrate that the synergy between TiO_2 and GQDs enhances photocatalytic performance under visible-light conditions, offering promising potential for environmental pollutant degradation.

4.3. Investigation of the Effects of TiO_2/GQDs Mass Ratio and Fe, Co, Ni, Mn Dopant Content on the Photocatalytic Properties of TiO_2/GQDs Composites

4.3.1. *Structure and Morphology*

XRD and BET analyses revealed changes in the crystal structure and an increase in specific surface area. Metal doping contributed to the formation of additional active sites and enhanced light absorption capability.

TiO_2/GQDs composites doped with Fe, Co, Ni, and Mn were successfully synthesized while maintaining the anatase phase, as confirmed by XRD and Raman analysis. BET results showed a high surface area and mesoporous structure, enhancing adsorption. FTIR confirmed Ti–O–C bonding, indicating GQD incorporation. UV–Vis spectra revealed a reduced band gap, especially at 12% doping, improving visible-light absorption.

Fe- and Co-doped TiO_2/GQDs composites exhibited superior photocatalytic activity, reducing MB concentration by ~65% after 4 hours—better than the undoped counterpart. The enhanced performance is attributed to the synergistic effect of GQDs and metal dopants, which suppress electron–hole recombination and boost visible-light-driven degradation efficiency.

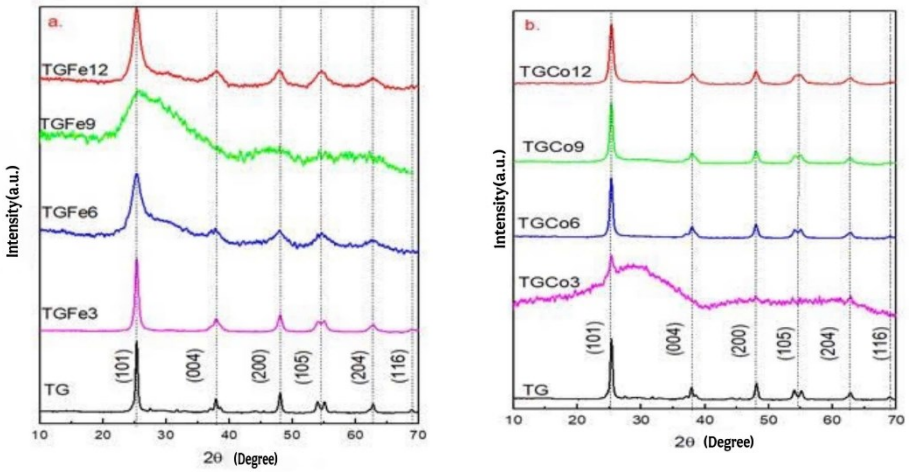

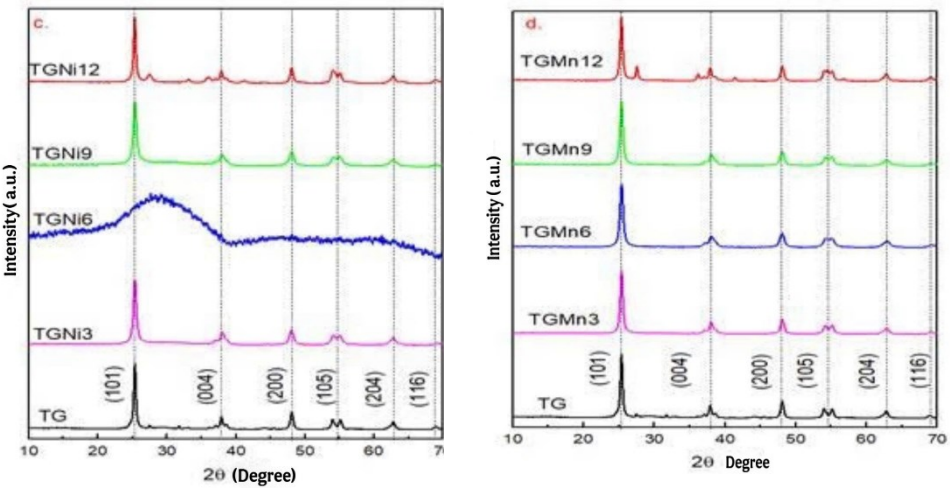

Figure 4.3. XRD patterns of the composite systems: (a) TiO_2/GQDs/Fe, (b) TiO_2/GQDs/Co, (c) TiO_2/GQDs/Ni, and (d) TiO_2/GQDs/Mn.

Chapter 4 – Conclusion

TiO_2/GQDs and metal-doped TiO_2/GQDs nanocomposites were successfully synthesized with good stability and strong photoluminescence. Metal doping reduced the band gap and improved visible-light absorption. Fe- and Co-doped samples (12%) showed the best photocatalytic activity due to efficient electron trapping and reduced charge recombination, highlighting their potential for visible-light-driven pollutant degradation.

CONCLUSIONS AND RECOMMENDATIONS

This dissertation focused on the synthesis, characterization, and evaluation of TiO_2/GQDs and Fe, Co, Ni, Mn-doped TiO_2/GQDs nanocomposites, aiming to enhance photocatalytic efficiency under visible light irradiation. Graphene was successfully exfoliated from graphite using a high-power ultrasonic device, offering an environmentally friendly and effective delamination process. GQDs were synthesized via pyrolysis of citric acid using microwave irradiation

(800 W, 4 min), followed by hydrothermal treatment at 220 °C for 16 hours at pH 11, resulting in highly uniform, strongly fluorescent quantum dots.

The integration of GQDs into TiO_2 led to a reduction in band gap from 3.22 eV to 3.05 eV and extended the absorption range into the visible spectrum. Raman, FTIR, and XRD analyses confirmed the presence of GQDs and the preservation of the anatase crystalline phase. Upon doping with transition metals—particularly Fe and Co at 12% loading—the band gap was further reduced to 2.42 eV and 2.97 eV, respectively, and the specific surface area increased, as evidenced by UV–Vis absorption and BET analyses. These doped materials exhibited enhanced light-harvesting ability and beneficial defect structures.

Photocatalytic degradation tests using methylene blue (MB) revealed that the TiO_2/GQDs (1:20) sample achieved the highest efficiency. Fe- and Co-doped samples demonstrated improved MB removal compared to pure TiO_2, due to the combined effects of electron transfer to GQDs and electron trapping by metal dopants. The proposed mechanism involves enhanced charge separation and prolonged charge carrier lifetime. The developed nanocomposites exhibited excellent chemical stability and high photocatalytic performance under simulated sunlight.

Recommendations for future work include extending the photocatalytic tests to a wider range of pollutants, integrating advanced treatment technologies, and evaluating real-world applicability. Additionally, further development of multifunctional materials is suggested, with potential applications in sensing, energy storage, and environmental remediation.

LIST OF PUBLICATION RELATED TO THE DISSERTATION

1. **Yen Hai Nguyen**, Phuong Thi Mai, Nghia Phan Trong Nguyen, Hau Van Tran, Hien Thi Minh Nguyen, Anh Thi Van Nguyen, Dung Viet Nguyen, Phuong Dinh Doan, Minh Ngoc Phan and Thang Hung Bui, 2024,

Fabrication of graphen from graphite using high – powered ultrasonic vibrators, *Materials Research Express*, 11, 025006.

2. Le Xuan Hung**, Nguyen Hai Yen**, Trinh Thi Hue, Dao Nguyen Thuan, Pham Nam Thang, Vu Thi Hong Hanh, Vu Cam Nhung, Julien Laverdant, Nguyen Thi Mai Huong and Pham Thu Nga, 2022, Fabrication and optical properties of sulfur and nitrogen doped graphene quantum dots by the microwave–hydrothermal approach, *Journal of Nanoparticle Research*, 24, 206.

3. **Nguyễn Hải Yến**, Mai Thị Phượng, Trần Văn Hậu, Nguyễn Cao Khang, Nguyễn Việt Dũng, Nguyễn Thị Ngọc Tú, Âu Thị Hằng, Tô Anh Đức, Phạm Văn Trình, Đoàn Đình Phương, Phan Ngọc Minh, Vũ Thị Thu Hà và Bùi Hùng Thắng, 2022, Nghiên cứu chế tạo vật liệu graphen từ graphit bằng thiết bị rung siêu âm công suất lớn, *Tạp chí Khoa học và Công nghệ Nhiệt đới*, 28, tr.113-121.

4**. Nguyễn Hải Yến**, Nguyễn Mạnh Hùng, Đào Việt Thắng, Phạm Lan Hương, Trần Thị Châm, Bùi Hùng Thắng, Nguyễn Cao Khang, 2021, Nghiên cứu chế tạo vật liệu chấm lượng tử Graphen, *Hội nghị Vật lý Chất rắn và Khoa học Vật liệu Toàn quốc – SPMS 2021*,2, tr. 989-992.

5. Le Xuan Hung, Pham Nam Thang, Dao Nguyen Thuan, Julien Laverdant, **Nguyen Hai Yen**, Phan Ngoc Hong, Trinh Thi Hue and Pham Thu Nga, 202, Synthesis, characterization and optical properties of heteroatom doping of graphen quantum dots, *Advances in Optics, photonics, Spectroscopy & Applications XI*, tr.110-116.

6. Le Xuan Hung, Trinh Thi Hue, **Nguyen Hai Yen**, Pham Nam Thang, Dao Nguyen Thuan, Julien Laverdant, Vu Cam Nhung and Pham Thu Nga, 2021, Doped graphen quantum dots: fabrication methods, optical properties and application prospects, *The 10th international workshop on advanced materials science and nanotechnology*, tr. 115-122.